NATIONAL ADVISORY COMMITTEE FOR AERONAUTICS

SPECIAL REPORT 123

TESTS OF SEVERAL MODEL NACELLE-PROPELLER ARRANGEMENTS IN FRONT OF A WING

By James G. McHugh
Langley Memorial Aeronautical Laboratory

September 1939

TESTS OF SEVERAL MODEL NACELLE-PROPELLER ARRANGEMENTS IN FRONT OF A WING

By James G. McHugh

SUMMARY

An investigation was conducted in the N.A.C.A. 20-foot wind tunnel to determine the drag, the propulsive and net efficiencies, and the cooling characteristics of several scale-model arrangements of air-cooled radial-engine nacelles and present-day propellers in front of an 18-percent-thick, 5- by 15-foot airfoil. Investigations of like arrangements simulating the geometric proportions of airplanes in the 20,000-pound weight classification have been conducted by the N.A.C.A. and the results are summarized in previous reports. This report deals with an investigation of wing-nacelle arrangements simulating the geometric proportions of airplanes in the 40,000- to 70,000-pound weight classification and having the nacelles located in the vicinity of the optimum location determined from the earlier tests.

Two 3-blade propellers with diameters of 36 and 48 inches, respectively, were each tested in conjunction with a 12-inch-diameter nacelle in three positions in front of the wing and with a 16-inch-diameter nacelle in six positions in front of the wing. Lift, drag, cooling-air flow, and propeller characteristics were determined for each of the arrangements. Comparisons on the basis of net efficiency between the various arrangements indicated that, for high-speed and cruising conditions, the most favorable location for a tractor nacelle-propeller arrangement of the type tested was with the thrust axis on the wing center line and with the propeller between 15 and 30 percent of the chord forward of the leading edge of the wing. The loss in net efficiency through the use of either large-diameter engines or nacelle installations having a high interference drag is clearly indicated.

In certain cases, the action of the propeller slipstream on the flow pattern over the wing-nacelle arrangement may be such as greatly to influence the cooling qualities of a given wing-nacelle-propeller arrangement.

INTRODUCTION

The design of engine-nacelle installations for large airplanes has always involved a certain amount of conjecture on the part of airplane designers. Several years ago the N.A.C.A. conducted a lengthy investigation for the purpose of establishing an optimum arrangement of the wing-nacelle-propeller combination (reference 1). That investigation covered a large range of variations in nacelle position and yielded results that have been of considerable value to designers. The tests of reference 1 were made with a nacelle of relatively large diameter as compared with the wing thickness, were conducted through a propeller operating range that would be used only in the take-off and climbing range of present-day airplanes, and did not include either a thorough investigation of the effects on net efficiency of small changes in nacelle location from the optimum location found nor measurements of cooling-air flow through the cowling.

In order to make a more detailed study of nacelle locations in the vicinity of the best position found in the previous test program and to investigate arrangements suitable for the 40,000- to 70,000-pound airplane classification, the N.A.C.A. has instituted an investigation in the 20-foot wind tunnel of wing-nacelle-propeller interference in which a wing, propellers, and engine-nacelle models simulating modern practice were used. The phases of the investigation that have been completed to date include (a) measurements of drag, propeller, and cooling characteristics for several combinations of geometrically similar propellers and nacelles of different nacelle-propeller diameter ratios with no wing present and (b) measurements of lift, drag, propeller, and cooling characteristics for the same nacelle-propeller combinations in several positions in front of a thick wing. Part (a) has been reported in reference 2; this report presents the results of part (b).

APPARATUS AND METHOD

The N.A.C.A. 20-foot wind tunnel in which these tests were conducted is described in detail in reference 3.

Two sheet-aluminum nacelles, 12 and 16 inches in diameter, were used in the investigation. The values of the

conductivity were 0.072 for the 12-inch nacelle and 0.085 for the 16-inch nacelle. The nacelles and the manner in which the engine was simulated are described in reference 2.

Two 3-blade propellers, 36 and 48 inches in diameter (reference 2), were used in the investigation. The blade angle of both propellers could be adjusted by turning the blades in the hub. For these tests, the blades were set at 25° and 35° at 0.75 of the tip radius. Additional tests of one of the arrangements were made with the propeller blades set at 15°, 20°, 30°, and 40° at 0.75 of the tip radius.

The electric motor used to drive the propeller is 10 inches in diameter and develops 25 horsepower at 3,600 r.p.m.

The wing used in the investigation has a span of 15 feet, a chord of 5 feet, and is of N.A.C.A. 23018 airfoil section. It was constructed of wood and was varnished and waxed to provide a smooth finish. The central portion of the wing was provided with suitable metal ribs and plates for the connections of the supports used in attaching the motor and the nacelle to the wing.

The wing was mounted on the standard balance supports described in reference 4. The arrangement was such that the wing could pivot about a line 25 percent of the chord back of the leading edge and 6 percent of the chord below the chord line. The angle of attack of the wing could be changed by an electric motor operating a worm to which the rear wing-support struts were attached. All forces acting on the wing were transmitted to a six-component automatic recording balance on the test-chamber floor.

Tests were made of nine wing-nacelle arrangements. Photographs of the arrangements are reproduced in figure 1 and the principal dimensions of each arrangement are given in figure 2. Figure 3 shows one of the wing-nacelle arrangements mounted in the tunnel for tests.

Each wing-nacelle arrangement was tested with the propeller removed. Measurements of lift, drag, pitching moment, and pressure drop through the cowling were made with the wing at an angle of attack of 3° and at air speeds varying from 20 to 100 miles per hour. In addition, each arrangement was tested at a constant air speed of 80 miles per hour and at wing angles of attack varying from -8° to

the angle of stall in increments of 1°. For use in subsequent analyses, similar tests were made of the wing alone.

A second series of tests was made of each combination with the propeller operating and with the wing at an angle of attack of 3°. The propeller speed was held constant and the air speed was increased by increments until a velocity of 80 miles per hour was reached; the air speed was then held constant and the propeller speed was varied to cover the rest of the propeller operating range. Simultaneous readings of torque, thrust, revolution speed, pressure drop through the cowling, lift, and air speed were taken at frequent intervals.

SYMBOLS AND COEFFICIENTS

The coefficients and symbols used in analyzing the results of this investigation are defined as follows:

q, dynamic pressure of air $(\frac{1}{2} \rho V^2)$.

ρ, mass density of air.

V, velocity of air stream.

n, propeller revolution speed.

L, lift.

D, drag.

ΔD, change in drag of nacelle due to propeller slipstream.

M, pitching moment about pivot.

T, thrust of propeller (tension in crankshaft).

R, net force on thrust balance.

D, diameter of propeller.

d, diameter of nacelle.

d/D, ratio of nacelle diameter to propeller diameter.

P, power supplied to propeller.

β, propeller blade angle at 0.75 of the tip radius.

S, area of wing.

c, chord of wing.

b, span of wing.

D_o, profile drag.

D_i, minimum induced drag $(L^2/\pi q b^2)$.

D_j, jet-boundary interference drag $\left(\delta \frac{L^2}{q \times \text{area of jet}}\right)$

where $\delta = 0.142$ for case under consideration (reference 5).

D_n, effective nacelle drag, drag of nacelle plus mutual wing-nacelle interference drag. at constant Lift.

ΔD_i, difference in induced drag of combination, at a given value of lift, from value of $L^2/\pi q b^2$ assumed for wing alone.

ΔD_j, difference in jet-boundary interference drag of combination, at a given value of lift, from value of $\delta \frac{L^2}{q \times \text{area of jet}}$ assumed for wing alone.

$D_L = D_i + D_j$

C_D, wing drag coefficient (D/qS).

C_{D_n}, effective nacelle drag coefficient $\left(\frac{D_n}{q(\pi d^2/4)}\right)$.

C_L, lift coefficient (L/qS).

C_m, pitching-moment coefficient (M/qSc).

C_T, propulsive thrust coefficient.

C_P, power coefficient $(P/\rho n^3 D^5)$.

V/nD, advance-diameter ratio of propeller.

η, propulsive efficiency $[(C_T/C_P)(V/nD)]$.

N.D.F., nacelle drag factor $(D_n V/P)$.

η_o, net efficiency $(\eta - \text{N.D.F.})$.

C_s, speed-power coefficient $(\sqrt[5]{\rho V^5/Pn^2})$.

Δp, pressure drop across engine.

$\sqrt{\Delta p/\rho n^2 D^2}$, cooling-air-flow coefficient.

Subscripts w, c, and p refer to conditions with wing alone, wing-nacelle combination, and wing-nacelle-propeller combination, respectively.

METHOD OF ANALYSIS

A discussion of the problems involved in evaluating the relative merits of wing-nacelle-propeller combinations is given in part VI of reference 1 and a method is therein derived for comparing the merits of the various arrangements at a constant value of the lift coefficient. Comparisons by that method necessitate conducting propeller tests at several angles of attack of the wing in order to obtain the power-on curves of lift coefficient against angle of attack for each arrangement.

The method of comparison used in the analysis of the results of the present investigation is basically similar to the one given in reference 1 except that, instead of comparing the various arrangements at a constant value of lift coefficient, they are compared at a constant angle of attack; the effect of variations in lift is eliminated by adding to the total drag of each arrangement the computed values of the change in minimum induced drag and wind-tunnel jet-boundary interference drag caused by the propeller. The necessity of obtaining the power-on curves of lift coefficient against angle of attack is thus eliminated and the amount of testing required is greatly decreased.

The derivation of the expressions for propulsive efficiency, net efficiency, and propulsive thrust coefficient follow.

The summation of horizontal forces acting on a nacelle-

propeller combination mounted on a balance in a wind tunnel is commonly written as follows:

$$R + D = T - \Delta D = \text{propulsive thrust}$$

where D is the drag with the propeller removed. The propulsive efficiency of the propeller-nacelle combination is defined as

$$\eta = \frac{(\text{propulsive thrust})\ V}{P} \tag{1}$$

When the propeller-nacelle unit is operating in proximity to a wing, the lift generated with the propeller operating is likely to differ from that generated at the same angle of attack with the propeller removed and on that account, unless proper precautions are taken in determining the value of the propulsive thrust to use in applying equation (1), an erroneous value of η may be obtained. In what follows, the method used to evaluate the propulsive efficiency, the net efficiency, and the propulsive thrust of the nacelle-propeller combination is explained.

The horizontal reaction of the wing alone on the balance supports, when tested in a circular open-throat wind tunnel, can be expressed as follows:

$$D_w = D_{o_w} + D_{i_w} + D_{j_w} \tag{2}$$

Similarly, the drag reaction of the wing-nacelle combination is

$$D_c = D_{o_w} + D_n + D_{i_c} + D_{j_c} + \Delta D_{i_c} + \Delta D_{j_c} \tag{3}$$

With the propeller operating, the horizontal reaction of the wing-nacelle-propeller combination is

$$R = T - \Delta D - D_{o_w} - D_n - D_{i_p} - D_{j_p} - \Delta D_{i_p} - \Delta D_{j_p} \tag{4}$$

Adding equations (3) and (4),

$$T - \Delta D = R + D_c + [(D_{i_p} + D_{j_p}) - (D_{i_c} + D_{j_c})] + [(\Delta D_{i_p} + \Delta D_{j_p}) - (\Delta D_{i_c} + \Delta D_{j_c})] \tag{5}$$

Equation (5) shows, for a given lift, a change from the computed values of induced and jet-boundary interference drag due to the effect of the propeller on the span load distribution. It is reasonable, therefore, to charge that drag to the propeller in determining its propulsive thrust. Thus,

$$\text{propulsive thrust} = (T-\Delta D) - [(\Delta D_{i_p}+\Delta D_{j_p}) - (\Delta D_{i_c}+\Delta D_{j_c})]$$

$$= (R+D_c) + [(D_{i_p}+D_{j_p}) - (D_{i_c}+D_{j_c})] \qquad (6)$$

The induced drag due to lift is

$$D_i = L^2/\pi q b^2 \qquad (7)$$

The jet-boundary interference drag is

$$D_j = \delta \frac{L^2}{q \times \text{area of jet}} \qquad (8)$$

where δ depends on the ratio of wing span to jet diameter and has a value of 0.142 for the case under consideration (reference 5).

Adding equations (7) and (8), introducing coefficients, and simplifying, includes tail 5.75°

$$D_L = D_i + D_j = 0.1402\ C_L^2\, qS \qquad (9)$$

If this expression is substituted in equation (6), the propulsive thrust is seen to be

$$T - \Delta D - [(\Delta D_{i_p} + \Delta D_{j_p}) - (\Delta D_{i_c} + \Delta D_{j_c})] =$$

$$= R + D_c + (D_{L_p} - D_{L_c}) \qquad (10)$$

Introducing coefficients and simplifying, express the propulsive thrust coefficient as

$$C_T = \frac{R + qS\,[C_{D_c} + 0.1402\ (C_{L_p}^2 - C_{L_c}^2)]}{\rho\, n^2\, D^4} \qquad (11)$$

The nacelle drag factor is defined as:

$$N.D.F. = D_n V/P \tag{12}$$

where D_n is the difference, at constant lift, between the drag of the combination and the drag of the wing alone. Equation (12) becomes, by introducing coefficients and simplifying,

$$N.D.F. = \left(\frac{C_{D_c} - C_{D_w}}{C_P}\right)\left(\frac{S}{2D^2}\right)\left(\frac{V}{nD}\right)^3 \tag{13}$$

The propulsive efficiency can be expressed as

$$\eta = \frac{C_T}{C_P}\frac{V}{nD} \tag{14}$$

and the net efficiency as

$$\eta_o = \eta - N.D.F. \tag{15}$$

Values of C_T, N.D.F., η, and η_o given in this report were computed according to the relations given in equations (11), (13), (14), and (15), respectively. The significance of η, η_o, and N.D.F. is fully discussed in reference 1, and the validity of the approximations involved in their determination is considered. Attention is called to the fact that, in this report, the value of η_o has been determined throughout the entire operating range for two blade-angle settings of the propeller; whereas, in reference 1, it was determined for only one blade-angle setting at values of V/nD of 0.42 and 0.65.

DISCUSSION OF RESULTS

The foregoing analysis shows that the essential factors influencing the merit of a wing-nacelle-propeller combination are: (a) the increase, at a given value of lift coefficient, in the drag of the wing-nacelle combination over the basic wing drag; and (b) the propulsive efficiency of the wing-nacelle-propeller combination. Theory indicates that the efficiency of the propeller is increased when it operates in the high-velocity region that exists above the wing (reference 6). Previous investigations have shown, however, that the increase in drag incurred by mount-

ing a conventional engine nacelle in any position such that the nacelle does not intersect the wing far offsets any gain in propulsive efficiency which may be obtained from such an arrangement. These investigations have also indicated that the minimum increase in drag due to the engine nacelle can be obtained only when the nacelle and the wing intersect in such manner that a large portion of the frontal area of the nacelle is common to the wing.

The results of the present investigation show the effect of small variations in nacelle location on effective nacelle drag and propulsive and net efficiencies when the nacelle is in the vicinity of its optimum location and, in addition, show the cooling-air-flow characteristics that were obtained with each arrangement.

Lift and Drag with Propeller Removed

The airfoil characteristics of the wing alone are compared with the corresponding characteristics of the various wing-nacelle combinations in figure 4. The angle of stall is seen to increase progressively as the nacelle is moved away from the wing. Any comparison of the effect of nacelle position on the maximum lift based on the results of these tests is of questionable value, however, because of secondary effects that are caused by the small span of the wing. Such effects at low lift coefficients will be of negligible magnitude and the comparison of effects that occur in the high-speed range ($C_L = 0.2$) is therefore valid.

From large-scale plots similar to those in figure 4, the value of effective nacelle-drag coefficient, i.e., the increase in drag coefficient caused by adding the nacelle to the wing, was determined by taking the difference, at constant lift coefficient, between the drag coefficient of the wing-nacelle combination and the drag coefficient of the wing alone. The variation of the effective nacelle drag in coefficient form based on the nacelle cross-sectional area according to the relation

$$C_{D_n} = (C_{D_c} - C_{D_w}) \frac{S}{\pi d^2/4}$$

is given as a function of the lift coefficient in figure 5. The results are not strictly comparable because, owing to the differences in cooling-air pressure drop shown in figure 6, the drag due to the cooling-air flow was not the

same for each arrangement tested. In order to place the values of effective nacelle drag on a more nearly comparable basis, the results of figure 5 were corrected to the condition of zero cooling-air flow according to the relation

$$C_{D_{n_o}} = C_{D_n} - K\,(\Delta p/q)^{3/2}$$

where $K(\Delta p/q)^{3/2}$ is the theoretical increase in drag coefficient due to the flow of air through the cowling (reference 2); $C_{D_{n_o}}$ is the effective nacelle drag coefficient for zero cooling-air flow; and K is the conductivity of the engine.

The variation of $C_{D_{n_o}}$ with C_L is given in figure 7. It is interesting to note that the minimum value of $C_{D_{n_o}}$ for the 16-inch nacelle is obtained with the nacelle centrally located with reference to the wing. No off-center locations were tested in the case of the 12-inch nacelle, but there is little likelihood that the drag could be materially reduced below the minimum value of $C_{D_{n_o}}$ of 0.025 obtained with that nacelle in the central location.

The effect of fore-and-aft location of the nacelle with reference to the wing is most clearly shown in figure 8. At a value of C_L of 0.2, the drag added by the 12-inch nacelle in the central location was practically independent of its distance from the wing. At the same value of C_L, the value of $C_{D_{n_o}}$ for the 16-inch nacelle was lowest at the 15-percent-chord position and increased with increasing distance from the wing. Lowering the 16-inch nacelle to positions 4, 5, and 6 gave the same general trend that occurred in the central location, but the drag was higher throughout the entire range.

At a value of C_L of 0.4, the lowest value of drag added by the 16-inch nacelle was obtained with the nacelle in the central location and close to the leading edge of the wing. The drag added by the same nacelle in the lower positions was practically uninfluenced by fore-and-aft location and was in all cases higher than the drag obtained in the central locations. In the case of the 12-inch nacelle in the central location, the drag was, for locations between

30 and 45 percent of the chord forward of the leading edge of the wing, nearly the same at a value of C_L of 0.4 as it was at 0.2 but, at the closer positions, the drag considerably increased at the higher value of C_L. The increase in drag with C_L that occurred in this case (12-inch nacelle in position 1) may have been due to the fact that the distance between the trailing edge of the cowling and the leading edge of the wing was short (fig. 1). It is conceivable that certain small interferences due to the flow around the juncture of the nacelle and the leading edge of the wing became more pronounced as the angle of attack of the wing was increased and thus increased the interference drag with increase in lift coefficient.

In general, the results indicate that, for high-speed flight conditions, it is desirable from considerations of drag to have the nacelle centrally located with reference to the wing and with the propeller axis approximately 15 percent of the wing chord forward of the leading edge of the wing.

The importance of nacelle diameter relative to wing thickness is shown in figure 9. This figure was derived from the results of the tests herein reported and from other tests of a complete model of a large airplane tested in the full-scale wind tunnel (reference 7). The effective nacelle drag coefficient decreases with relative nacelle diameter until the nacelle diameter becomes equal to the wing thickness. Beyond that point, however, further decrease in relative nacelle size causes practically no change in the effective nacelle drag coefficient.

Careful filleting at the juncture of the wing and the nacelle is of prime importance. The comparison in figure 7 of tests made with the 16-inch nacelle in position 3 with two different fairing arrangements indicates the importance of good intersections. The two fillets were similar except that fillet A did not expand the air on the upper surface as rapidly as did fillet B. Fillet A also had numerous surface irregularities; whereas fillet B was quite smooth. The surface irregularities of fillet A apparently accounted for an increase in nacelle drag of nearly 30 percent in the range of lift coefficients corresponding to high-speed flight. At high values of C_L, the drag obtained with fillet A became less than that obtained with fillet B. This decrease may have been due to the fact that the lower rate of expansion of fillet A prevented separa-

tion, and attendant increase in drag, from occurring at the higher values of C_L.

Propulsive and Net Efficiency

The results of tests with the propeller operating were reduced to the conventional coefficient form and plotted as a function of V/nD. Figure 10 is given as a sample. Presentation of the results in their entirety is unwarranted; consequently, only that part required for final analysis is included. Values of C_T, C_P, η, η_o, and C_s read from carefully faired curves at even values of V/nD have been tabulated and can be obtained on request from the N.A.C.A.

The envelope curves of net and propulsive efficiency obtained from tests of the various arrangements are given in figures 11 and 12. Comparison of the results is simplified through the use of the cross plots of η given in figures 13 and 14 and the cross plots of η_o given in figures 15 and 16. Inspection of these curves reveals that, when the nacelle was centrally located with reference to the wing, the propulsive efficiency was not greatly affected either by variation in fore-and-aft location or by variation in the value of d/D, the maximum value of η being between 0.80 and 0.835 for all the arrangements tested with the nacelle in the central location.

The effect of variation in d/D on propulsive efficiency appeared to be more pronounced for the off-center nacelle locations. In the case of the 48-inch propeller operating in conjunction with the 16-inch nacelle, i.e., d/D = 0.33, the variation with fore-and-aft location was small, being of the order of 1 percent; but, in the case of the 36-inch propeller operating in front of the same nacelle, i.e., d/D = 0.44, the propulsive efficiency was from 2 to 5 percent lower than that obtained with the value of d/D of 0.33 and there was a marked tendency for η to decrease as the distance of the propeller from the wing was increased. Thus, it is seen that, for the central nacelle locations, the wing has a tendency to neutralize the effects of d/D on η but, for the off-center locations, the effect of the wing is less pronounced and the variation of η with d/D is almost as great as that obtained from the tests of nacelles alone (reference 2).

The maximum value of η has already been shown to be but slightly affected by nacelle location; the nacelle drag was therefore the factor with the most influence on η_o. Comparison of the curves of net efficiency given in figures 15 and 16, together with the curves of propulsive efficiency given in figures 11 and 12 and the values of effective nacelle drag coefficient given in figure 8, shows the relative importance of nacelle drag and propulsive efficiency on the net efficiencies of the various wing-nacelle-propeller arrangements. The highest values of net efficiency were obtained with the arrangements that gave the lowest nacelle drag, i.e., the 12-inch nacelle in the central locations; and the lowest values of net efficiency were obtained with the arrangements that gave the highest nacelle drag, i.e., the 16-inch nacelle in the off-center locations.

The trend of the curves of η_o given in figures 15 and 16 indicates that, for all the arrangements tested, the best location was in the position of lowest drag, that is, with the nacelle centrally located with respect to the wing thickness and with the propeller between 15 and 30 percent of the chord ahead of the leading edge of the wing.

The data in figures 15 and 16 show the effect of variations in nacelle drag to be much more pronounced at high than at low values of d/D. This fact is evident when it is considered that the net thrust T_o is equal to the propulsive thrust minus the effective nacelle drag.

The nacelle drag expressed as a percentage of the propulsive thrust increases with the ratio d/D. Inasmuch as η_o depends directly on T_o, a given percentage change in the value of D_n will have a much greater influence on η_o at high than at low values of d/D. This effect is clearly illustrated by the comparison given in figure 17 of the results obtained from tests of two different fillet arrangements on the same nacelle.

Lift and Pitching Moment with Propeller Operating

The effects of the operating propeller on the lift and the pitching-moment coefficients are shown in figures 18 and 19, respectively. Faired curves showing the mean of all values of these coefficients are given. Bracketing curves denote the maximum variation of the test points from

the mean value. The results shown in figures 18 and 19 are applicable only to the particular arrangements tested in this investigation and are included to show that, except at low values of C_s, the effect of the variables considered in this investigation on the lift and the pitching-moment coefficients is small.

Cooling Characteristics

The results obtained from measurements of the pressure drop through the engine cowling are presented in figures 20 and 21. The method of presentation is the same as that used in reference 2, where it is discussed in detail.

The change in cooling-air-flow characteristics with change in the ratio of nacelle diameter to propeller diameter (figs. 20 and 21) is in agreement with the results of determinations of cooling-air-flow characteristics of nacelles alone reported in reference 2 in that, when the nacelle diameter is large relative to the propeller diameter, the cooling-air flow with the propeller operating is considerably greater than when the nacelle diameter is small relative to the propeller diameter. Further comparison of figure 20 with the results shown in figure 16 of reference 2 reveals that, in the case of the 16-inch nacelle, the action of the propeller was to increase the cooling-air flow above that obtained with the propeller removed when the nacelle was in the presence of the wing; whereas the results of tests of the nacelle alone (reference 2) indicate that, except at low values of V/nD, the action of the propeller reduced the air flow through the cowling. Similar comparisons show that, in the case of the 12-inch nacelle, the propeller reduced the cooling-air flow when the nacelle was in the presence of the wing and that the effect was more pronounced than shown by tests of the same nacelle alone. Further inspection of figures 20 and 21 shows that moving the 12-inch nacelle closer to the wing caused the action of the propeller to become more detrimental to the cooling-air flow but that, as the 16-inch nacelle was moved closer to the wing, the action of the propeller on the cooling-air flow became increasingly advantageous. This apparent inconsistency is not clearly understood. The effect of the propeller on the cooling-air flow is probably dependent on the flow conditions that exist around the nacelle in front of the wing. It is therefore possible that the change in flow around the nacelles as they were moved closer to the wing allowed the

propeller to magnify its distorting effect on the flow in such a manner as to improve the cooling-air flow of the 16-inch nacelle and to impair the cooling-air flow of the 12-inch nacelle.

CONCLUSIONS

1. The effect of variation in the ratio of nacelle diameter to propeller diameter on the propulsive efficiency of a wing-nacelle-propeller combination is dependent on the location of the nacelle relative to the wing. When the nacelle is located directly in front of the wing, the effect is small; when the nacelle is lowered to a position such that the thrust axis becomes tangent to the lower surface of the wing, the effect becomes more pronounced. In all cases, however, the effect is smaller in magnitude than was shown from tests of nacelles alone.

2. The highest net efficiency was obtained with the arrangement that gave the lowest drag, that is, with the nacelle centrally located with respect to the wing and with the propeller axis about 15 percent of the wing chord ahead of the leading edge of the wing.

3. The propeller slipstream had but little effect on the lift and the moment coefficients of the wing in the range of cruising-speed lift coefficients.

4. The action of the propeller on the cooling-air flow is dependent both on the size and on the position of the nacelle relative to the wing.

Langley Memorial Aeronautical Laboratory,
National Advisory Committee for Aeronautics,
Langley Field, Va., May 31, 1939.

REFERENCES

1. Tests of Nacelle-Propeller Combinations in Various Positions with Reference to Wings.

   Part I. Thick Wing - N.A.C.A. Cowled Nacelle - Tractor Propeller, by Donald H. Wood. T.R. No. 415, N.A.C.A., 1932.

   II. Thick Wing - Various Radial-Engine Cowlings - Tractor Propeller, by Donald H. Wood. T.R. No. 436, N.A.C.A., 1932.

   III. Clark Y Wing - Various Radial-Engine Cowlings - Tractor Propeller, by Donald H. Wood. T.R. No. 462, N.A.C.A., 1933.

   IV. Thick Wing - Various Radial-Engine Cowlings - Tandem Propellers, by James G. McHugh. T.R. No. 505, N.A.C.A., 1934.

   V. Clark Y Biplane Cellule - N.A.C.A. Cowled Nacelle - Tractor Propeller, by E. Floyd Valentine. T.R. No. 506, N.A.C.A., 1934.

   VI. Wings and Nacelles with Pusher Propeller, by Donald H. Wood and Carlton Bioletti. T.R. No. 507, N.A.C.A., 1934.

2. McHugh, James G., and Derring, Eldridge H.: The Effect of Nacelle-Propeller Diameter Ratio on Body Interference and on Propeller and Cooling Characteristics. T.R. No. 680, N.A.C.A., 1939.

3. Weick, Fred E., and Wood, Donald H.: The Twenty-Foot Propeller Research Tunnel of the National Advisory Committee for Aeronautics. T.R. No. 300, N.A.C.A., 1928.

4. Wood, Donald H.: Tests of Large Airfoils in the Propeller Research Tunnel, Including Two with Corrugated Surfaces. T.R. No. 336, N.A.C.A., 1929.

5. Theodorsen, Theodore, and Silverstein, Abe: Experimental Verification of the Theory of Wind-Tunnel Boundary Interference. T.R. No. 478, N.A.C.A., 1934.

6. Weiselsberger, C.: Contribution to the Mutual Interference of Wing and Propeller. T.M. No. 754, N.A.C.A., 1934.

7. Silverstein, Abe, and Wilson, Herbert A., Jr.: Drag and Propulsive Characteristics of Air-Cooled Engine-Nacelle Installations for Large Airplanes. T.R. (to be published), N.A.C.A., 1939.

FIGURE LEGENDS

The 16-inch nacelle; position 1	The 16-inch nacelle; position 2	The 16-inch nacelle; position 3
The 16-inch nacelle; position 4	The 16-inch nacelle; position 5	The 16-inch nacelle; position 6
The 12-inch nacelle; position 1	The 12-inch nacelle; position 2	The 12-inch nacelle; position 3

Figure 1.- Wing-nacelle arrangements tested.

Figure 2.- Dimensions of arrangements tested.

Figure 3.- Set-up in tunnel for test. The 16-inch nacelle; position 5.

(a) The 12-inch nacelle; positions 1, 2, and 3.
(b) The 16-inch nacelle; positions 1, 2, and 3.
(c) The 16-inch nacelle; positions 4, 5, and 6.

Figure 4.- Comparison of lift and drag characteristics of wing alone with various wing-nacelle combinations.

Figure 5.- Variation of effective nacelle drag coefficient with lift coefficient. Cooling-air flow through nacelle as indicated by figure 6.

Figure 6.- Variation of $\Delta p/q$ with lift coefficient. Propeller removed.

Figure 7.- Variation of effective nacelle drag coefficient with lift coefficient. Corrected to zero cooling-air flow.

Figure 8.- Variation of effective nacelle-drag coefficient with nacelle location. Corrected to zero cooling-air flow.

Figure 9.- Variation of effective nacelle drag coefficient with the ratio of wing thickness to nacelle diameter. Propeller axis at 25 percent of the chord forward of the leading edge of the wing; zero cooling-air flow; α, 0°.

Figure 10.- Typical propeller curves with test points. The 16-inch nacelle in position 2; 48-inch propeller.

Figure 11.- Envelope curves of net and propulsive efficiencies against C_s. The 36-inch propeller; net efficiency corrected to zero cooling-air flow; α, 3°.

Figure 12.- Envelope curves of net and propulsive efficiencies against C_s. The 48-inch propeller; net efficiency corrected to zero cooling-air flow; α, 3°.

Figure 13.- Variation of propulsive efficiency with nacelle location at constant values of C_s. The 36-inch propeller; α, 3°.

Figure 14.- Variation of propulsive efficiency with nacelle location at constant values of C_s. The 48-inch propeller; α, 3°.

Figure 15.- Variation of net efficiency with nacelle location at constant values of C_s. The 36-inch propeller; net efficiency corrected to zero cooling-air flow; α, 3°.

Figure 16.- Variation of net efficiency with nacelle location at constant values of C_s. The 48-inch propeller; net efficiency corrected to zero cooling-air flow; α, 3°.

Figure 17.- Envelope curves of net and propulsive efficiencies showing the effect of fillets. The 16-inch nacelle; net efficiency corrected to zero cooling-air flow; α, 3°.

Figure 18.- Effect of propeller and nacelle location on lift coefficient. Value of C_L for wing alone, 0.190; α, 3°.

Figure 19.- Effect of propeller and nacelle location on pitching-moment coefficient. Value of C_m for wing alone, 0.005; α, 3°.

(a) Position 1; (b) Position 2; (c) Position 3
(d) Position 4; (e) Position 5; (f) Position 6
Figure 20.- Variation of $\sqrt{\Delta p/\rho n^2 D^2}$ with V/nD for various wing-nacelle-propeller arrangements tested. The 16-inch nacelle; conductivity, 0.085.

(a) Position 1; (b) Position b; (c) Position 3
Figure 21.- Variation of $\sqrt{\Delta p/\rho n^2 D^2}$ with V/nD for various wing-nacelle-propeller arrangements tested. The 12-inch nacelle; conductivity, 0.072.

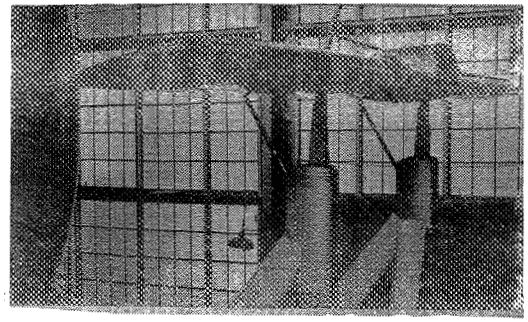

16-INCH NACELLE; POSITION 1

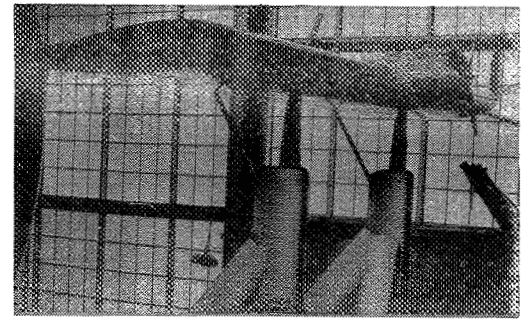

16-INCH NACELLE; POSITION 2

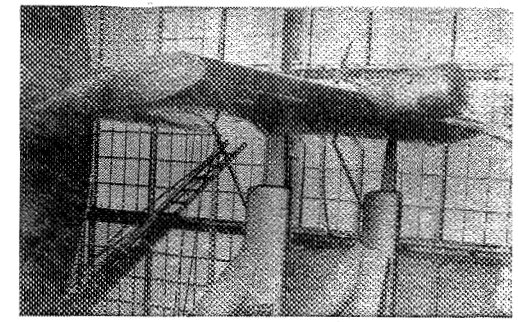

16-INCH NACELLE; POSITION 3

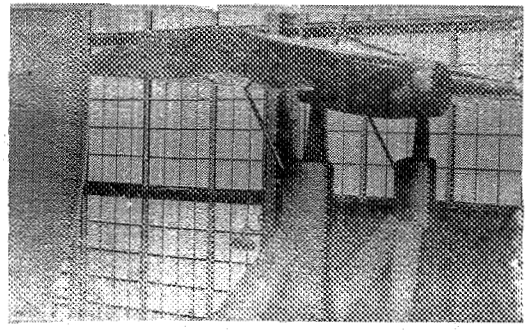

16-INCH NACELLE; POSITION 4

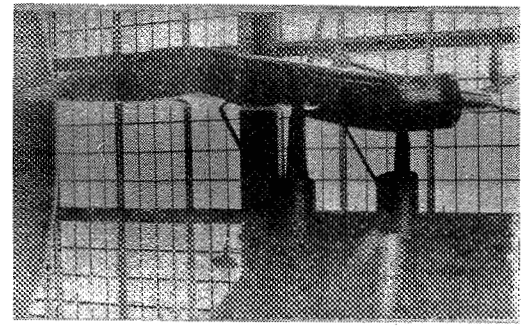

16-INCH NACELLE; POSITION 5

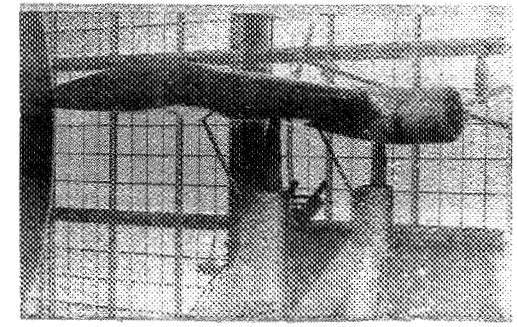

16-INCH NACELLE; POSITION 6

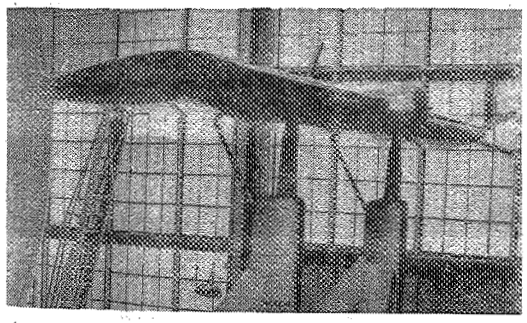

12-INCH NACELLE; POSITION 1

12-INCH NACELLE; POSITION 2

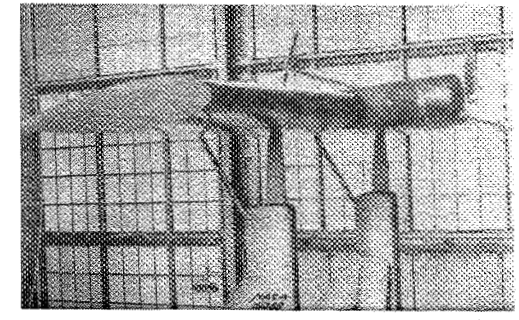

12-INCH NACELLE; POSITION 3

NACA
16755

Figure 1

NACA

Fig. 1

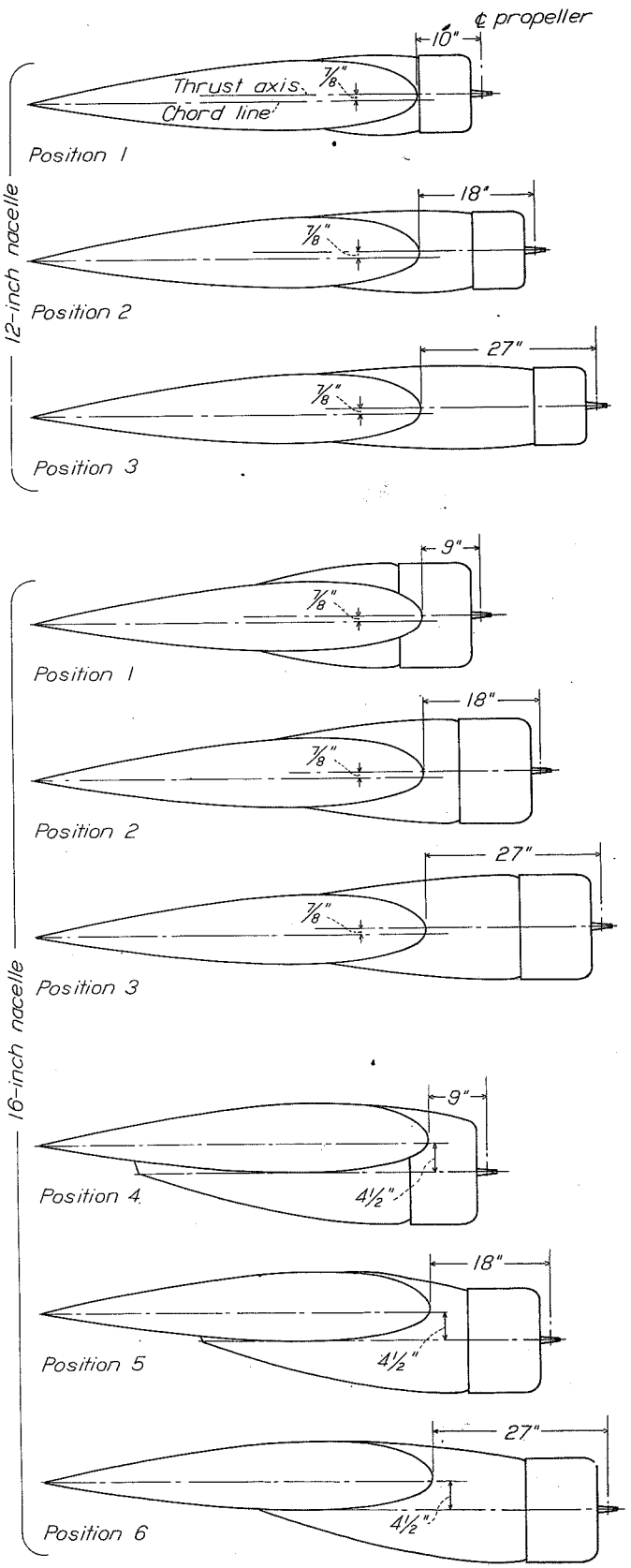
℄ propeller
10"
Thrust axis
Chord line
7/8"
Position 1
18"
7/8"
Position 2
27"
7/8"
Position 3
12-inch nacelle
9"
7/8"
Position 1
18"
7/8"
Position 2
27"
7/8"
Position 3
16-inch nacelle
9"
4½"
Position 4
18"
4½"
Position 5
27"
4½"
Position 6

Figure 2

Figure 3

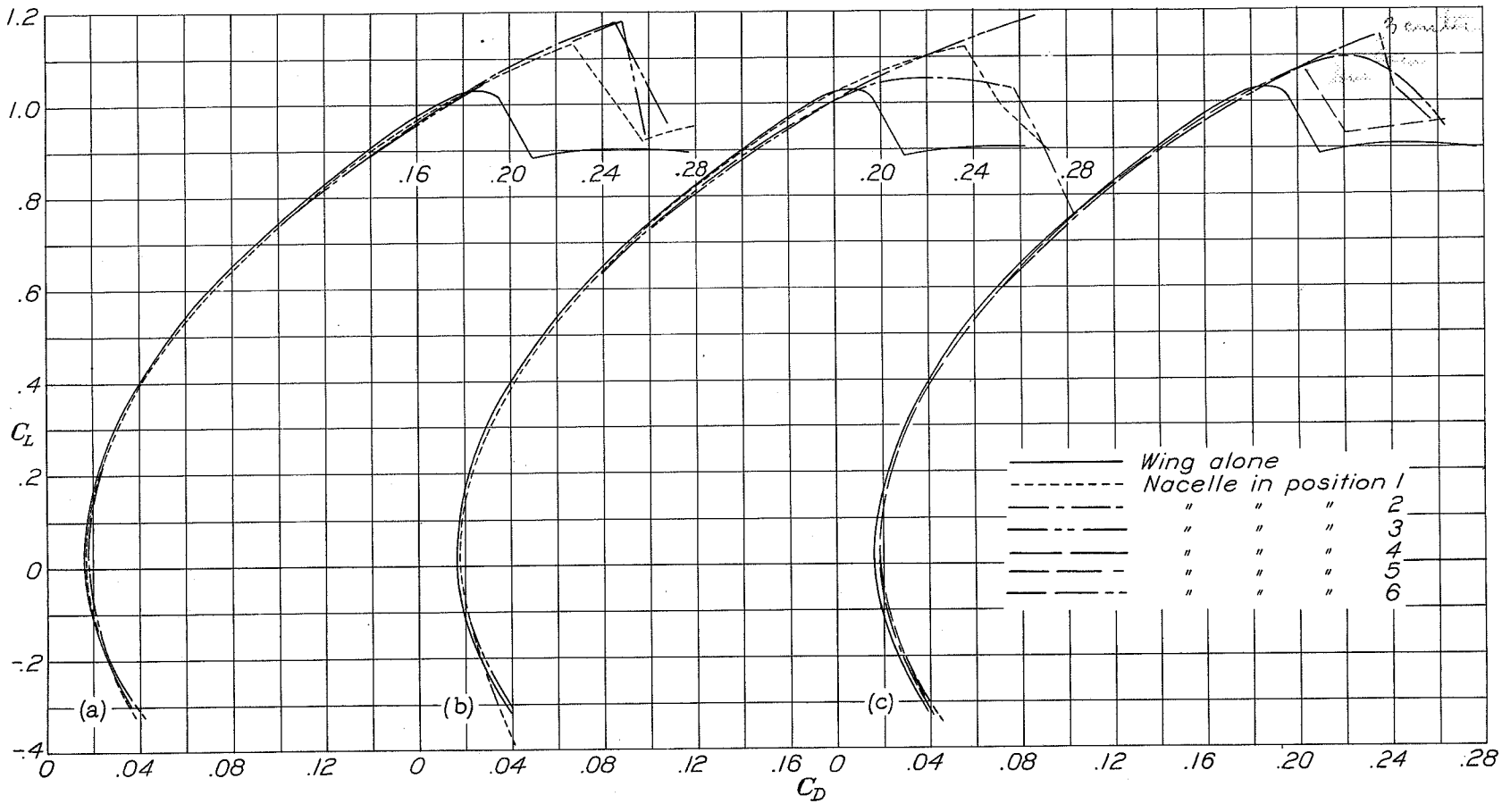
1.2
1.0
.8
.6
.4
C_L
.2
0
-.2
-.4
0
.04
.08
.12
.16
.20
.24
.28
C_D
(a)
(b)
(c)
Wing alone
Nacelle in position 1
" " " 2
" " " 3
" " " 4
" " " 5
" " " 6

Figure 4

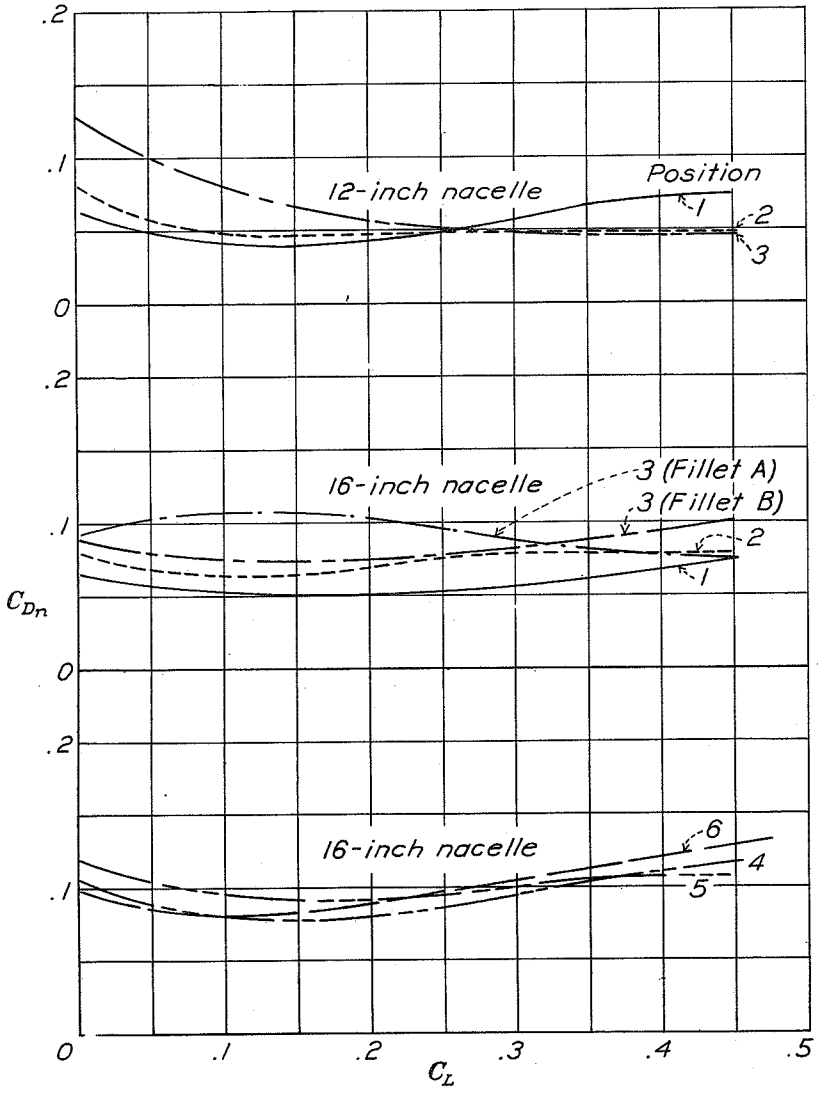

Figure 5.

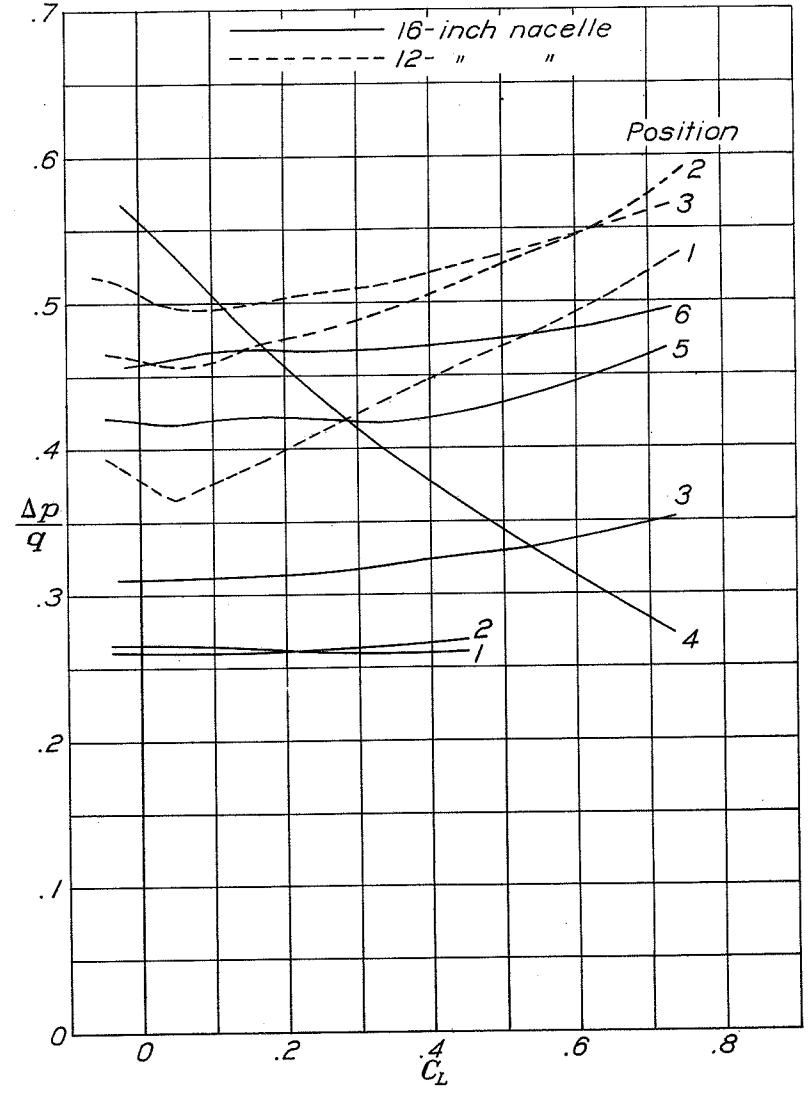

Figure 6

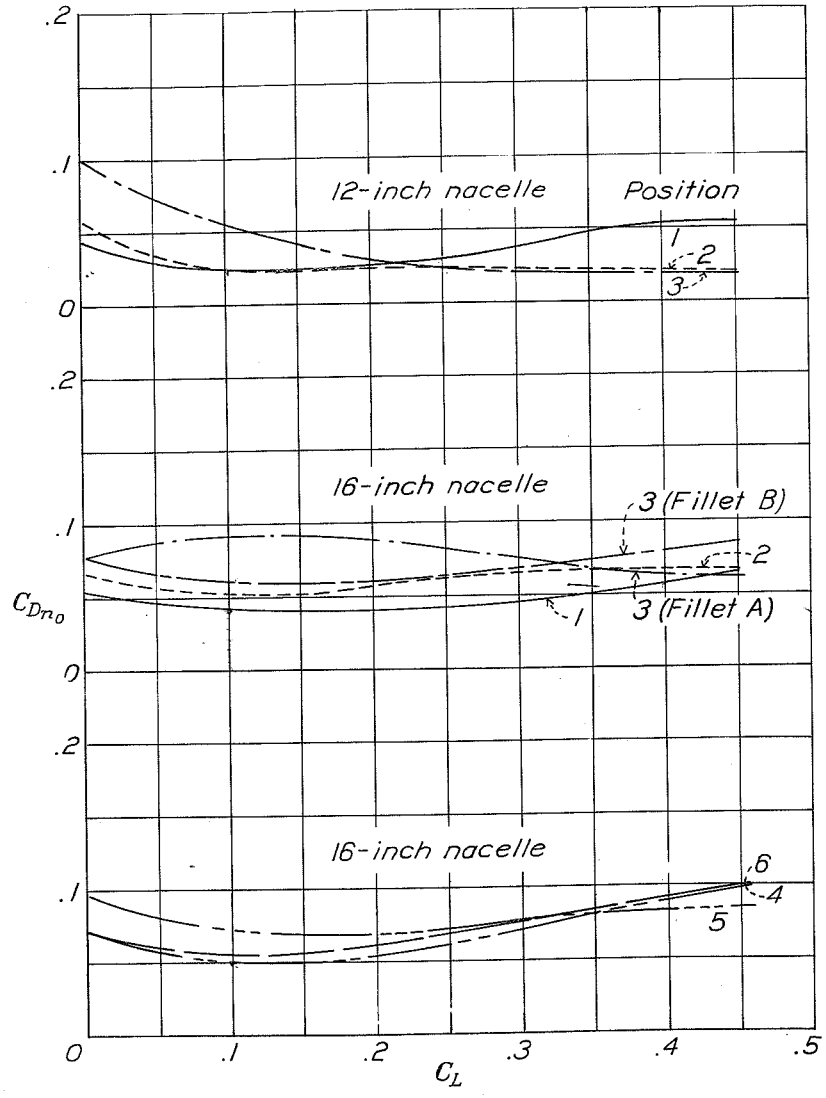

Figure 7

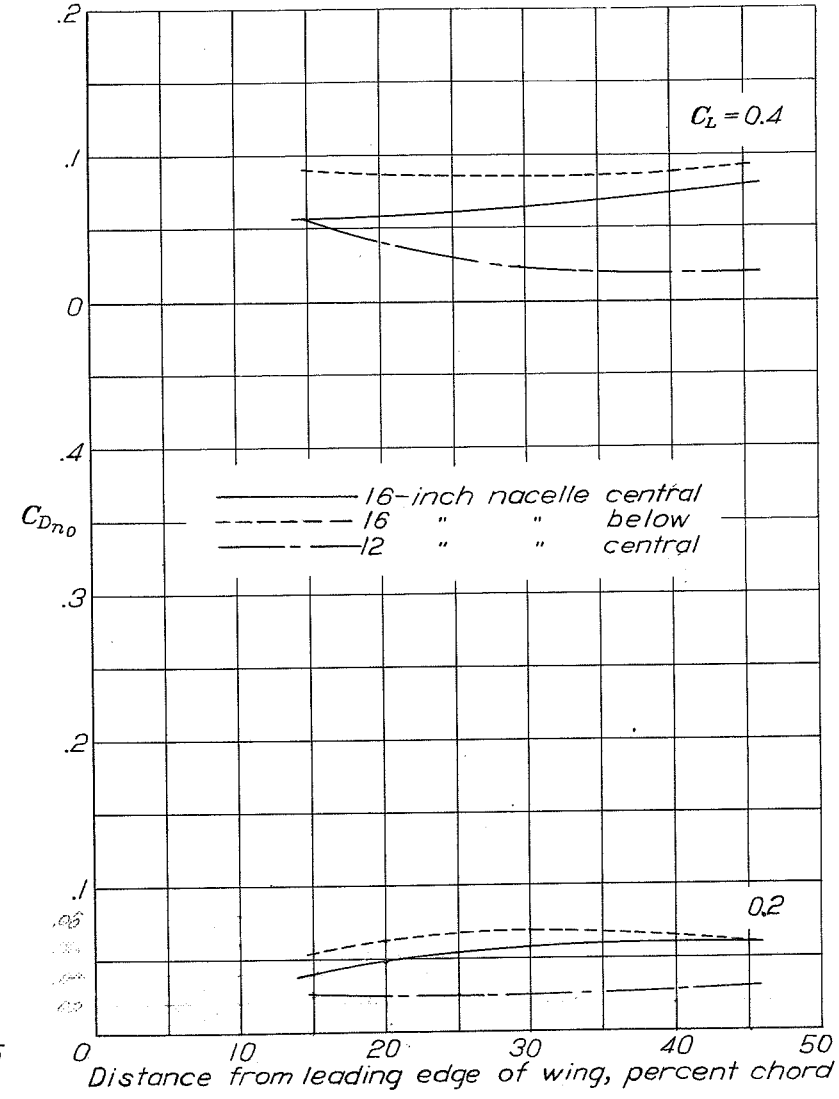

Figure 8

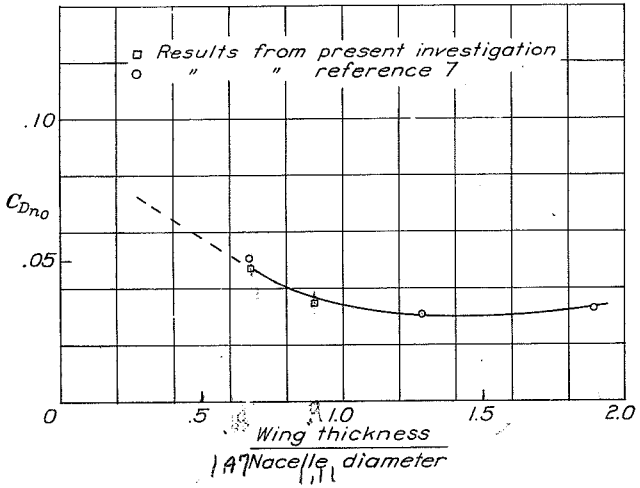

Figure 9.

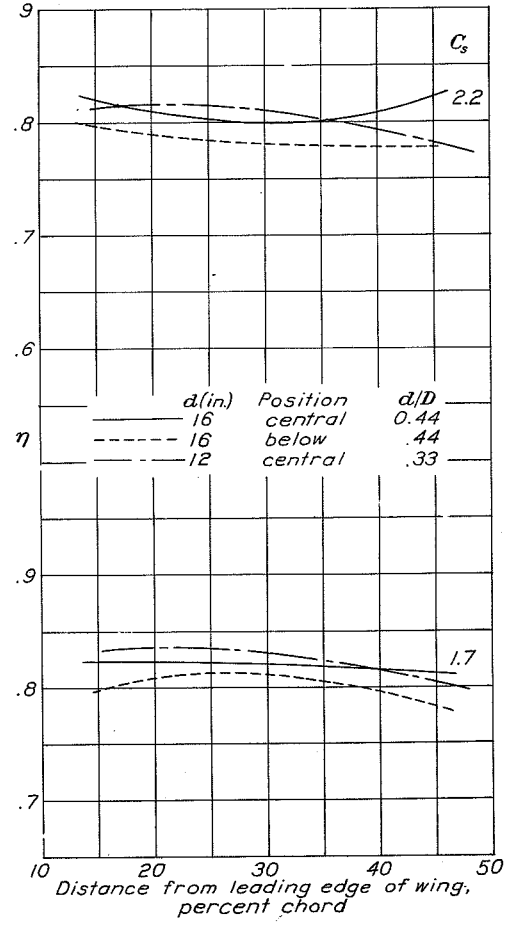

Figure 13.

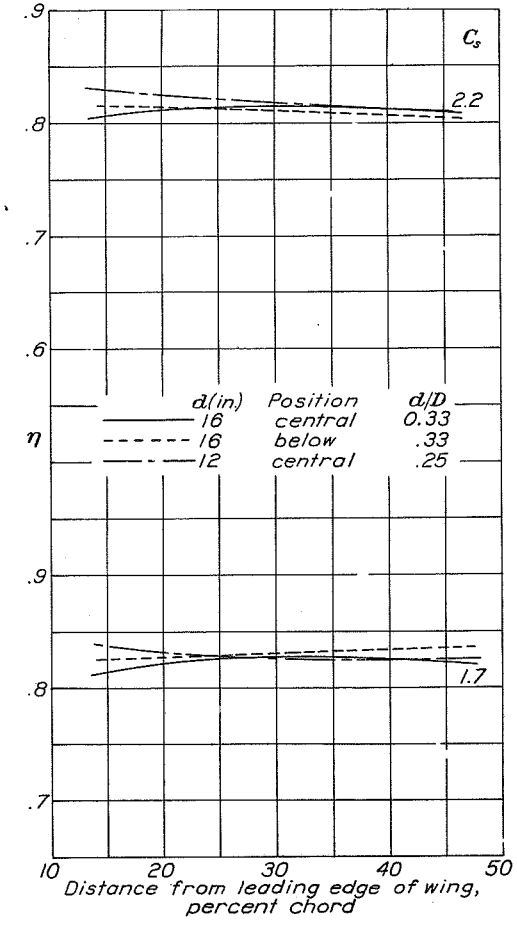

Figure 14

N.A.C.A.

Figs. 9, 13, 14

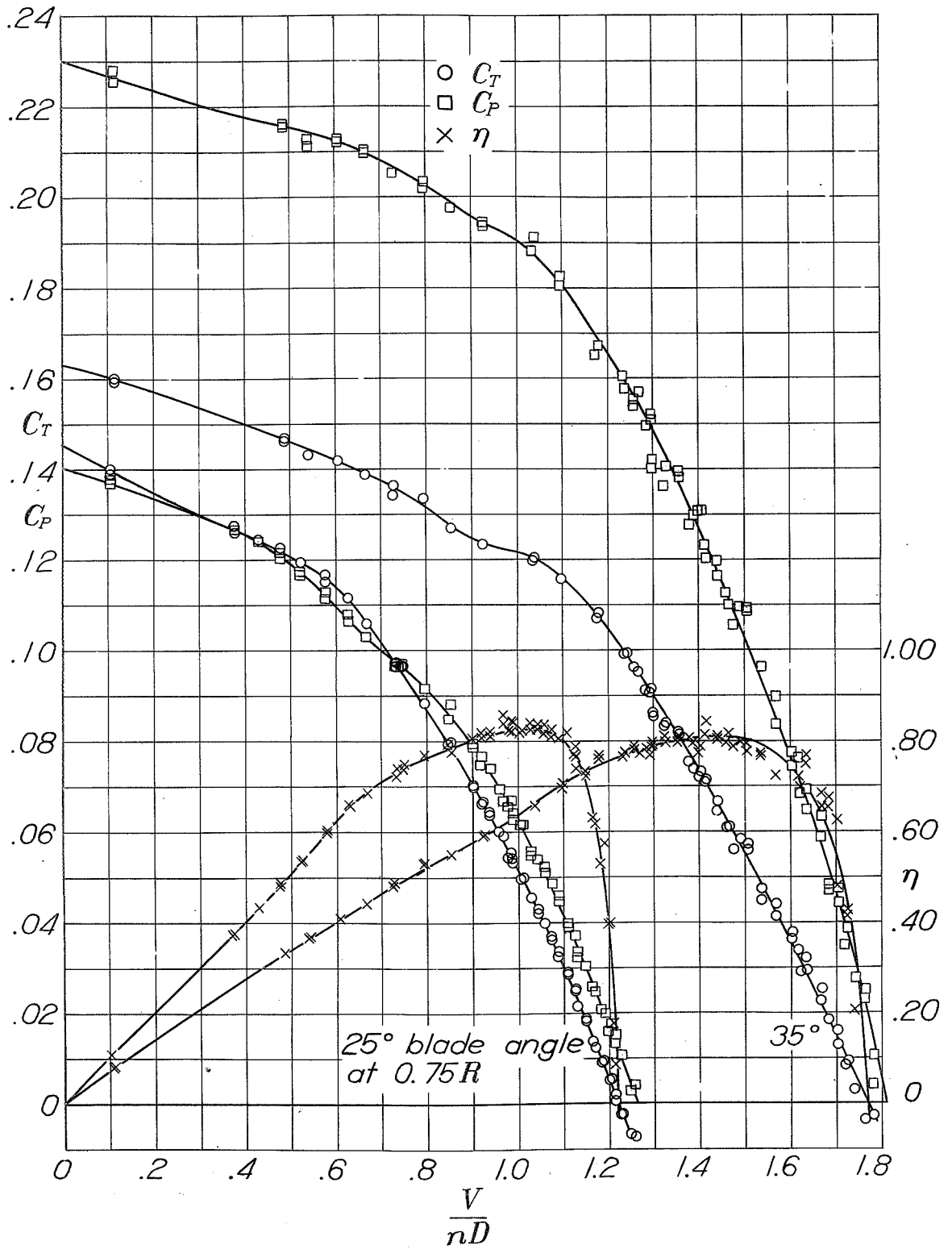
.24
.22
.20
.18
.16
C_T
.14
C_P
.12
.10
.08
.06
.04
.02
0
C_T
C_P
η
1.00
.80
.60
η
.40
.20
0
25° blade angle at 0.75R
35°
0
.2
.4
.6
.8
1.0
1.2
1.4
1.6
1.8
$\frac{V}{nD}$

Figure 10

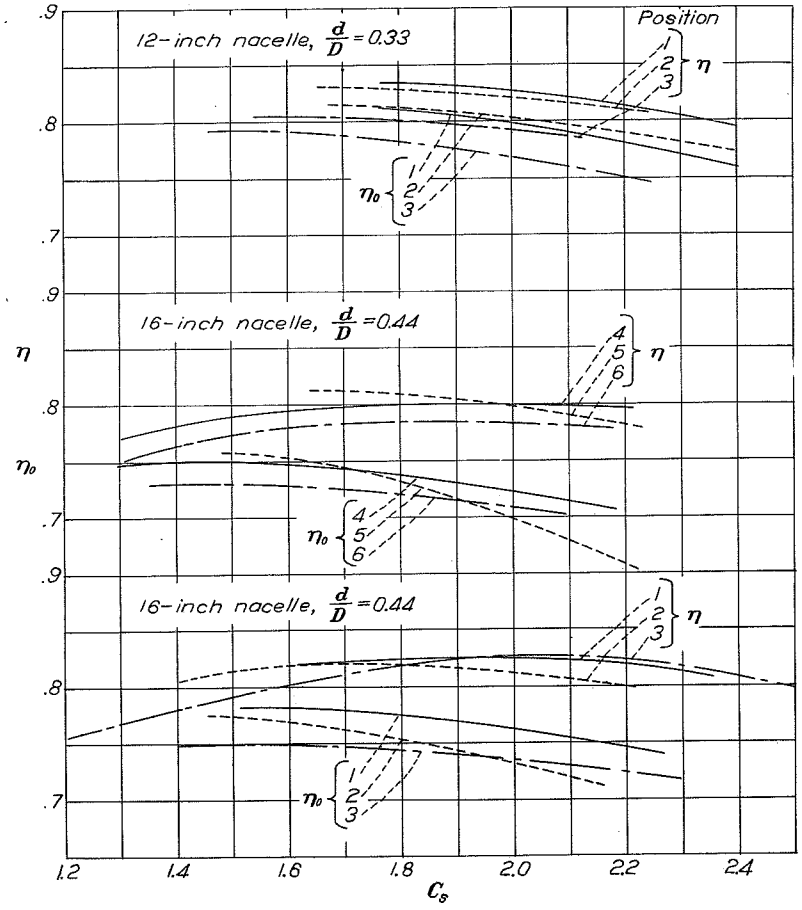

Figure 11

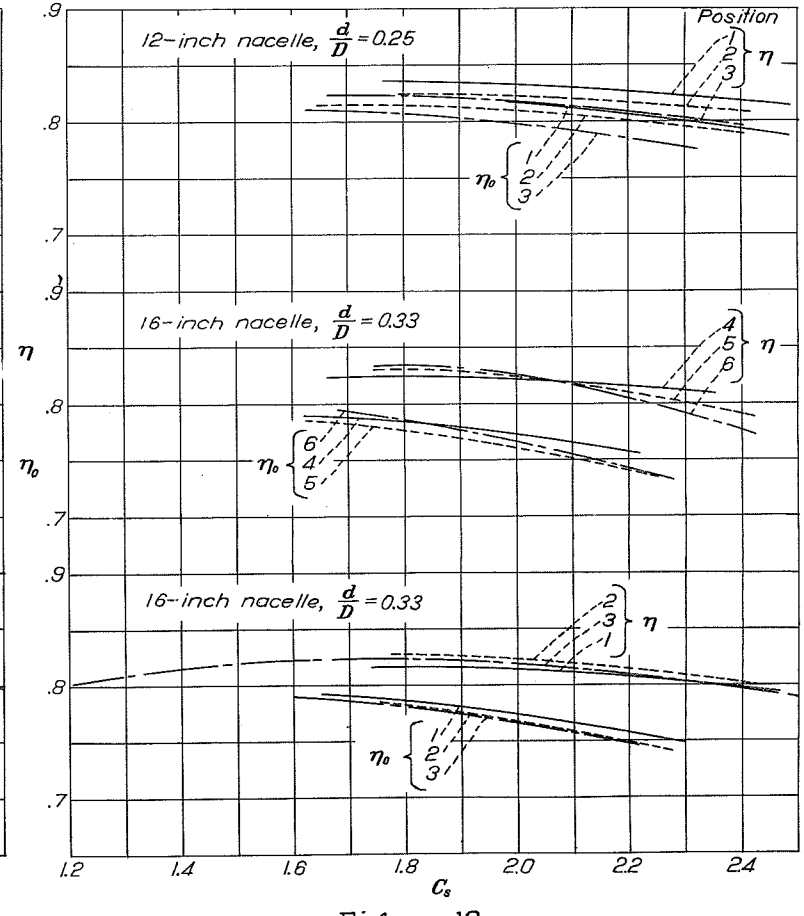

Figure 12

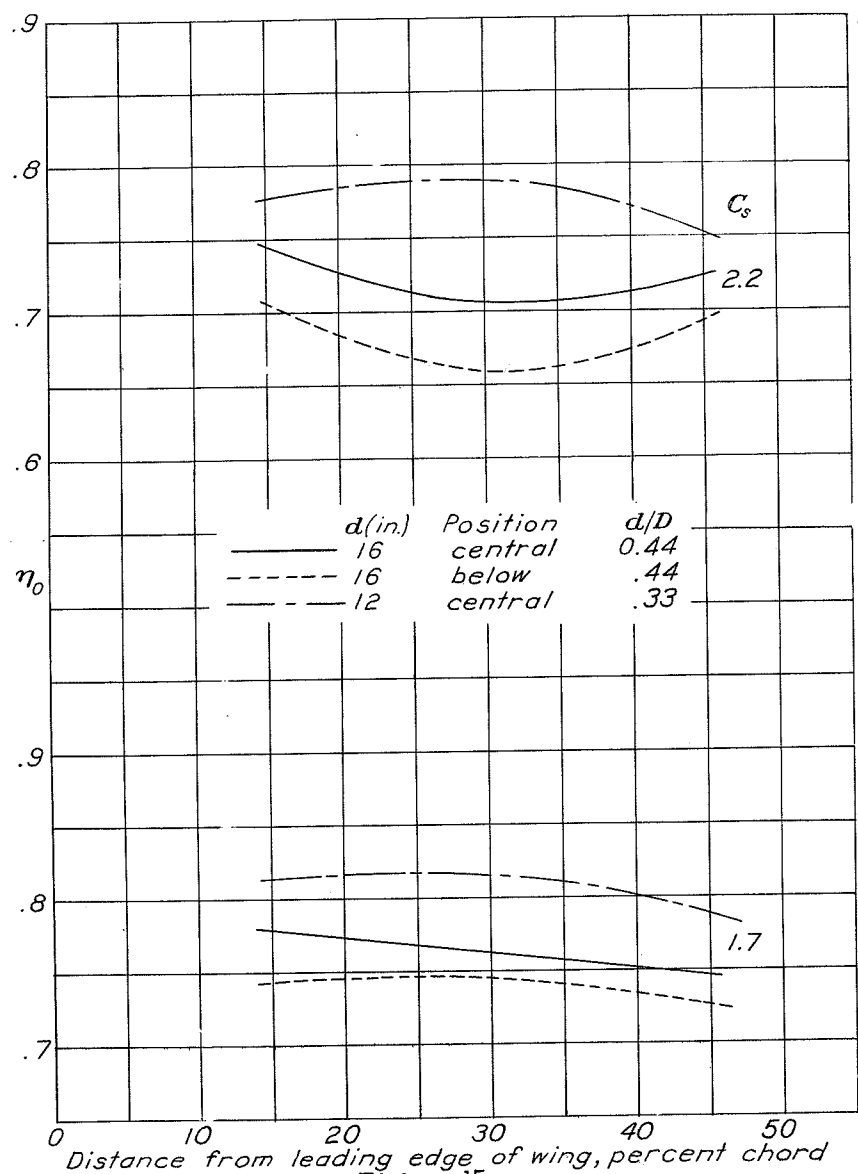

Figure 15

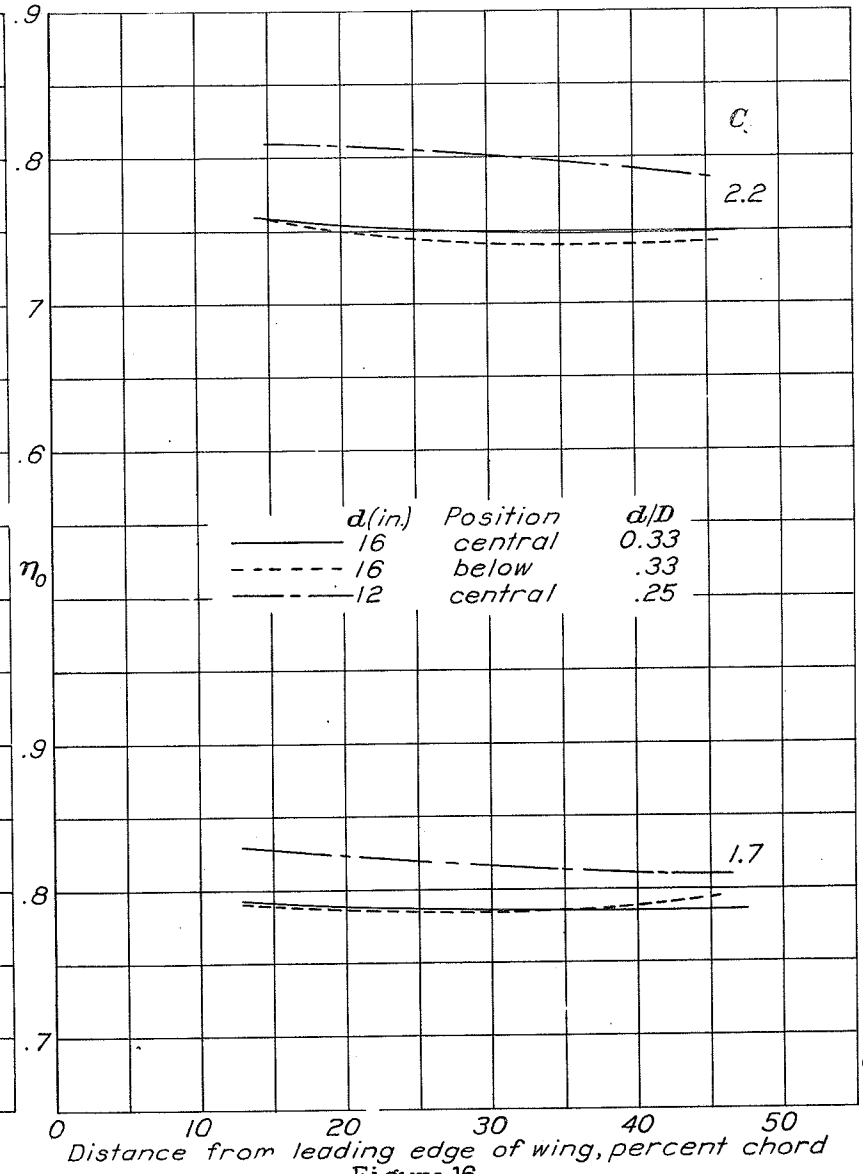

Figure 16

Figs. 17, 18, 19

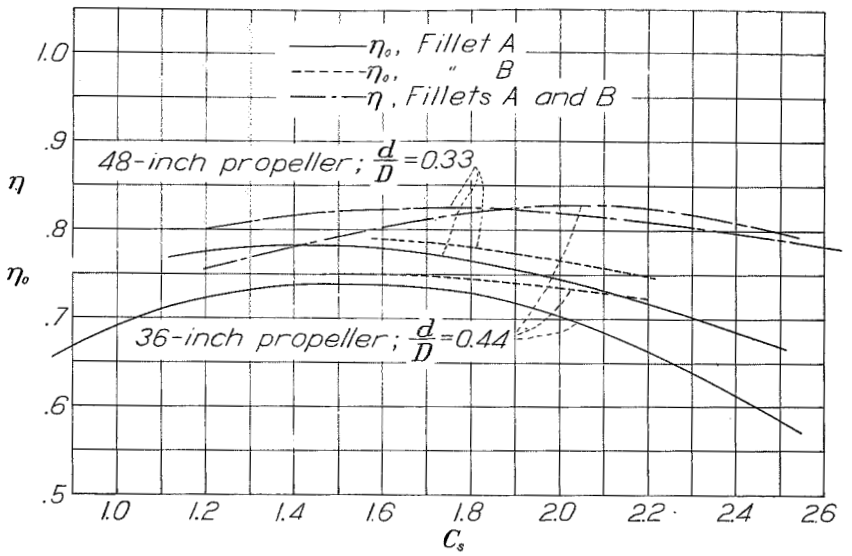

Figure 17

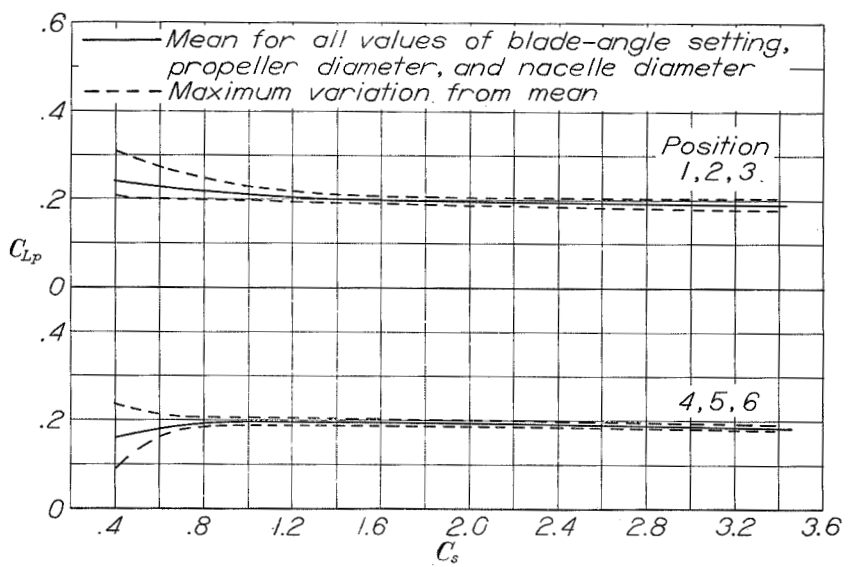

Figure 18

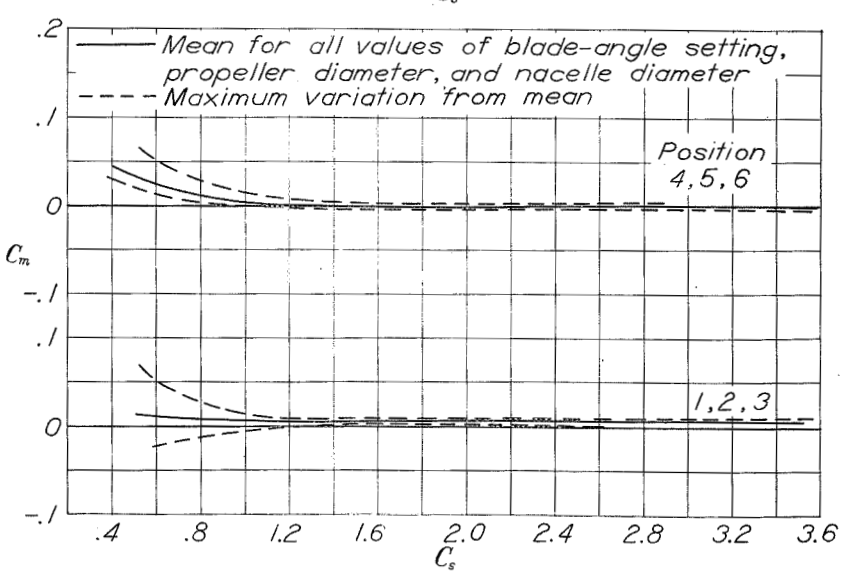

Figure 19

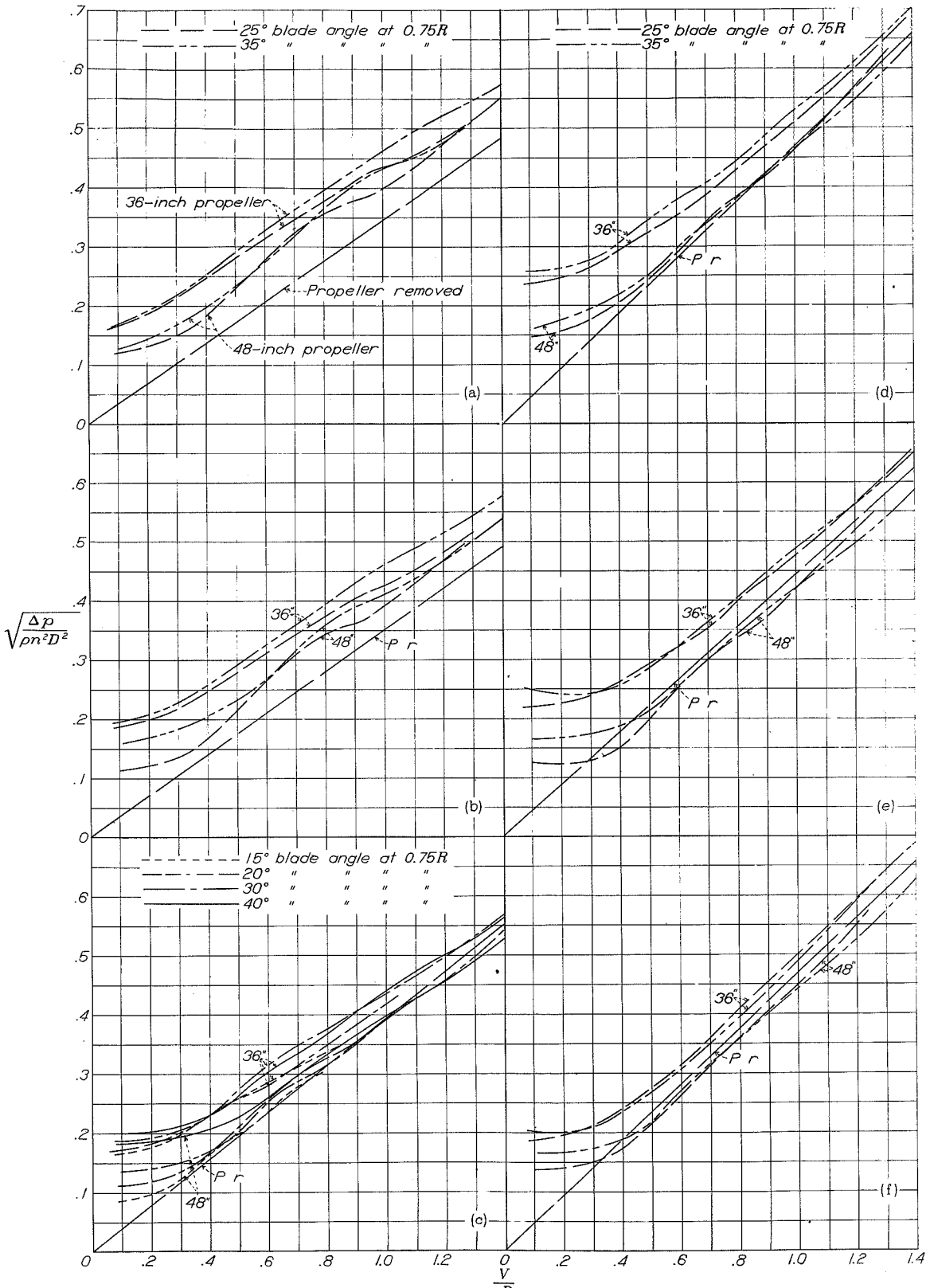
25° blade angle at 0.75R
35° " " " "
36-inch propeller
Propeller removed
48-inch propeller
(a)
(d)
36"
48"
P r
(b)
(e)
15° blade angle at 0.75R
20° " " " "
30° " " " "
40° " " " "
(c)
(f)
$\sqrt{\frac{\Delta p}{\rho n^2 D^2}}$
$\frac{V}{nD}$
0 .2 .4 .6 .8 1.0 1.2 1.4

Figure 20

N.A.C.A.

Fig. 21

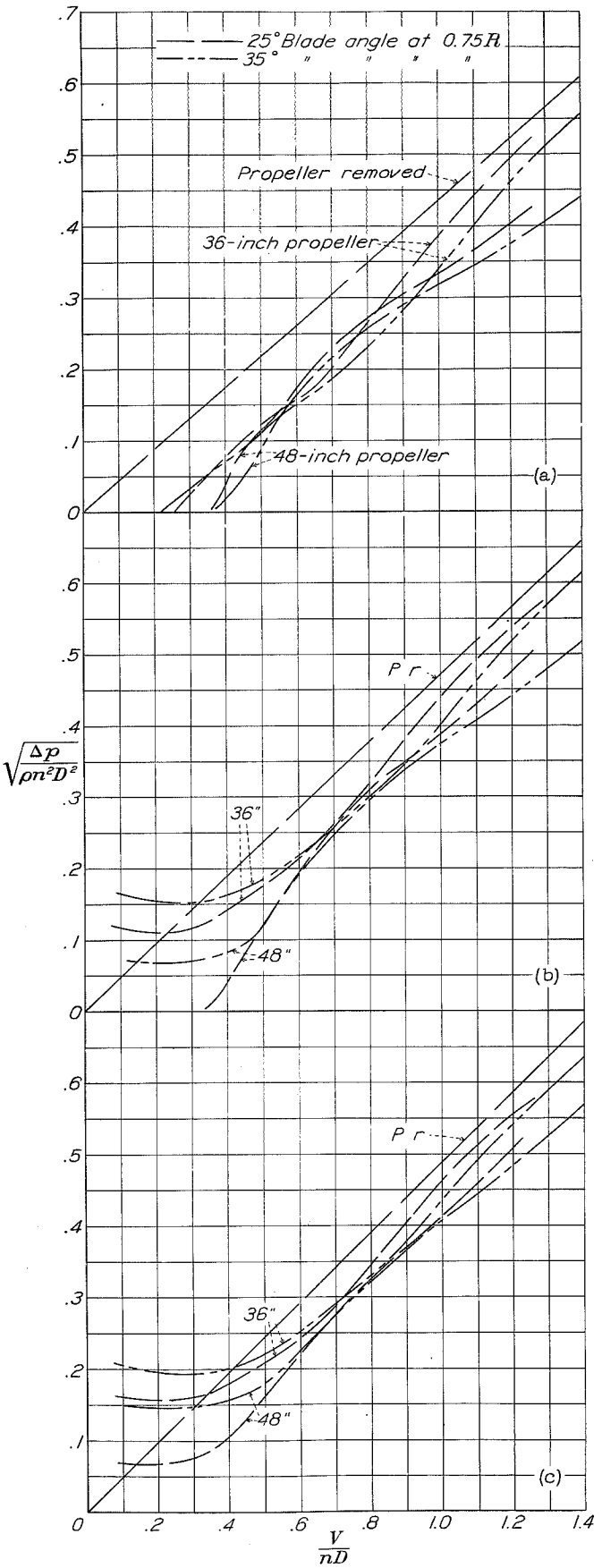

Figure 21